PR
https://www.jstage.jst.go.jp/browse/prpsj
DOI: https://doi.org/10.2517/prpsj.240029
Paleontological Research, vol. 30, p. 28–45, 2026
Article

Quaternary benthic foraminifera of core PC311 atop a seamount in the Magellan Seamounts (western Pacific Ocean)

Hiroyuki TAKATA[1,2†], Hiroki HAYASHI[3], Seiji HORIUCHI[4], Ritsuo NOMURA[5], Chan Min YOO[6], Boo-Keun KHIM[7*]

[1]*BK21 School of Earth and Environmental Systems, Pusan National University, 2 Busandaehak-ro 63 beon-gil, Busan 46241, Korea*
[2]*Estuary Research Center, Shimane University, 1060 Nishikawatsu, Matsue 690-8504, Japan*
[3]*Institute of Environmental Systems Science, Shimane University, 1060 Nishikawatsu, Matsue, Shimane 690-8504, Japan*
[4]*Palynosurvey, Co. Ltd, 559-3 Okanogou, Fujioka, Gunma 103-0023, Japan*
[5]*Faculty of Education, Shimane University, 1060 Nishikawatsu, Matsue, Shimane 690-8504, Japan*
[6]*Ocean Georesources Research Department, Korea Institute of Ocean Science and Technology, 385 Haeyang-ro, Busan 49111, Korea*
[7]*Department of Oceanography and Marine Research Institute, Pusan National University, 2 Busandaehak-ro 63 beon-gil, Busan 46241, Korea*

[Received November 14, 2024; Revised manuscript accepted December 7, 2025; Published online March 30, 2026]

ABSTRACT

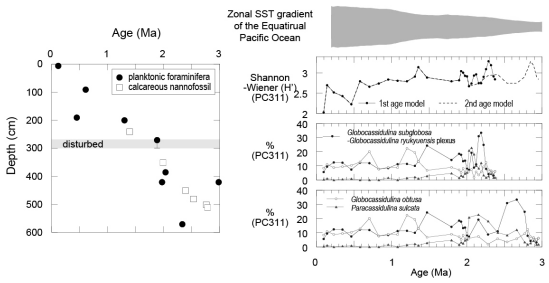

We examined biostratigraphic age inferences based on planktonic foraminifera and calcareous nannoplankton and documented the faunal associations of benthic foraminifera during the Quaternary in core PC311 taken from the top of a seamount (1,370 m water depth) in the Magellan Seamounts (western Pacific Ocean). Six and five biostratigraphic datums were recognized by planktonic foraminifera and calcareous nannofossils, respectively. In the lower part of the core, a planktonic foraminiferal datum occurred at the depth corresponding to 2.332 Ma, whereas the two datums of calcareous nannofossils were observed at 2.76 Ma and 2.78 Ma. As a result, we propose two age models. The diversity measures of benthic foraminifera declined gradually from ~1.3 Ma to the present. Stilostomellidae and Pleurostomelidae also decreased gradually after ~1.3 Ma and disappeared at ~0.7 Ma, as taxa went extinct across the Mid-Pleistocene Transition. In contrast, *Pseudoparrella obtusa*, a possible phytodetritus species, increased intermittently after ~1.3 Ma. In the lower part of the core, *Globocassidulina subglobosa–Globocassidulina ryukyuensis* plexus were abundant before ~1.5 Ma, whereas *Globocassidulina obtusa* became common after ~1.4 Ma. The faunal transition in core PC311 from the seamount top in the western Pacific Ocean appears to be related to the enhanced zonal gradient of sea surface temperature between the eastern and western Equatorial Pacific Ocean at ~1.3 Ma as well as the changes in global deep-water circulation including the persistent North Pacific Deep Water and/or the Upper Circumpolar Deep Water from the Southern Ocean-originated deep water.

Keywords: benthic foraminifera, biostratigraphy, calcareous nannoplankton, equatorial east-west temperature gradient, faunal transition, planktonic foraminifera

Introduction

Northern Hemisphere glaciation (NHG) marked an important global cooling event during the Cenozoic (Lyle *et al.*, 2008; Fedorov *et al.*, 2015). During this cooling trend, the meridional and equatorial gradients of sea surface temperature (SST) developed into an important climatic driver (e.g. Fedorov *et al.*, 2015). In contrast, during the Late Neogene, the closing of the Indonesian Seaway and the Panama Isthmus was crucial for warming conditions in the western Pacific Ocean through the evolution of the Kuroshio Current (Lyle *et al.*, 2008). These tectonic

* Corresponding author: Boo-Keun KHIM (bkkhim@pusan.ac.kr)
† Present address: Faculty of Dinosaur Paleontology, Fukui Prefectural University, 4-1-1 Kenjojima, Matsuoka, Eiheiji, Fukui 910-1195, Japan

events led to the eventual development of the present-day Western Pacific Warm Pool (Lyle *et al.*, 2008). The warmer SST condition in the eastern and western Equatorial Pacific Ocean during the Early Pliocene, known as "Permanent El Niño", is markedly different from that of the modern ocean (Wara *et al.*, 2005), whereas the Early-to-Middle Pleistocene transition represented an enhancement of the zonal SST gradient between the eastern and western Equatorial Pacific Ocean (e.g. Fedorov *et al.* 2015).

During the Early Pliocene, the temporal development of the Pacific Meridional Overturning Circulation (PMOC) (e.g. Motoi *et al.*, 2005) was reported in the transient deep-water formation of the North Pacific Deep Water (NPDW) (Burls *et al.*, 2017). Based on a neodymium isotope study of the carbonate fraction, Le Houedec *et al.* (2016) suggested that the NPDW was formed on the Ontong-Java Plateau (Ocean Drilling Program (ODP) Site 807) in the western Equatorial Pacific Ocean) during the Early Pliocene. During the same period, Feng *et al.* (2022) suggested the transient formation of NPDW based on the carbon isotope composition of benthic foraminifera at ODP Site 807. However, limited evidence of deep-water circulation at intermediate depths in pelagic settings has hampered our understanding of PMOC development.

The major extinction of deep-sea benthic foraminiferal taxa occurred during the Mid-Pleistocene Transition (MPT: ~1.25–0.70 Ma; Pisias and Moore, 1981) (e.g. Thomas, 2007; Hayward *et al.*, 2012). Therefore, it is imperative to constrain the timings of taxon disappearances at various locations and depths. Furthermore, the diversification of Cassidulinidae has also occurred since the start of the Pleistocene (e.g. Nomura, 1983b). Thus, it is important to document the extinction/diversification processes of deep-sea benthic foraminifera at low-latitude bathyal depths in the western Pacific Ocean and consider possible relationships with global climate changes, such as the east-west SST gradient and global deep-water circulations.

In this study, we examined biostratigraphic age inferences based on planktonic foraminifera and calcareous nannoplankton and documented the faunal associations of benthic foraminifera during the Quaternary in core PC311 which was collected from the bathyal depth (1,370 m) of the Magellan Seamounts (western Pacific Ocean). These results contribute to our understanding of paleoceanographic changes not only in the surface ocean, but also in the deep ocean of the low-latitude pelagic setting of the subtropical western Pacific Ocean.

Study area and materials

Low-latitude regions in the western Equatorial Pacific Ocean are characterized by warm surface water, the North and South Equatorial Currents (NEC and SEC, respectively) and trade winds (e.g. Wyrtki, 1974; Li and Fedorov, 2022). The salinity front is formed between the NEC and North Pacific Gyre (NPG) owing to precipitation with the Intertropical Convergence Zone (ITCZ) in the western Pacific Ocean (e.g. Kao and Lagerloef, 2015) (Supplementary figure 1). The salinity front, which is usually positioned at ~15°N, is affected by seasonal variability and the El Niño-Southern Oscillation (Kao and Lagerloef, 2015). The chlorophyll-a concentration in the surface water of the study area is low because of the latitudinal distance from the equatorial wind-driven mixing zone (Supplementary figure 1). The abyssal depths in the western Pacific Ocean are largely bathed by Upper Circumpolar Deep Water (UCDW), which originates from the Southern Ocean (Reid, 1997). In contrast, the North Pacific Intermediate Water (e.g. Reid, 1965) has been strongly developed, particularly during glacial periods, originating from the high-latitude areas in the North Pacific Ocean, including the Bering Sea and Okhotsk Sea.

Piston core PC311 (598 cm in length) was collected from a seamount top (17°0.559′N, 152°1.907′E; 1,370 m water depth; Figure 1) of the Magellan Seamounts in the western Pacific Ocean. The core site is located at the boundary between the NEC and NPG. The lithology consists primarily of homogeneous and sometimes burrowed calcareous oozes without marked sedimentary structure. Samples were collected at 1-cm intervals, with the exception of the soupy top part of the core (5–0 cm). Core sediments in the 298–268 cm interval were disturbed during core handling. All samples were freeze-dried, and an aliquot of approximately 1–6 g of sediment was collected every 10 cm for foraminiferal analysis (62 samples). In addition, 44 samples (approximately 1 g) were collected separately from the lower part of the core at depths ranging from 598 cm to 235 cm for calcareous nannofossil analysis.

Methods

Benthic foraminifera

After being weighed, the 62 samples collected at ~10-cm intervals from 598.5–2.5 cm for foraminiferal analysis were soaked in warm water and wet-sieved using a 63-μm sieve. The residues were dried at 50°C, then re-weighed to calculate the %coarse fraction (>63 μm) and split into 1/2 to 1/32 aliquots. More than 200 benthic foraminiferal specimens were picked, identified and counted in the >105 μm fractions of 32 samples at approximately 20-cm intervals using a binocular microscope following

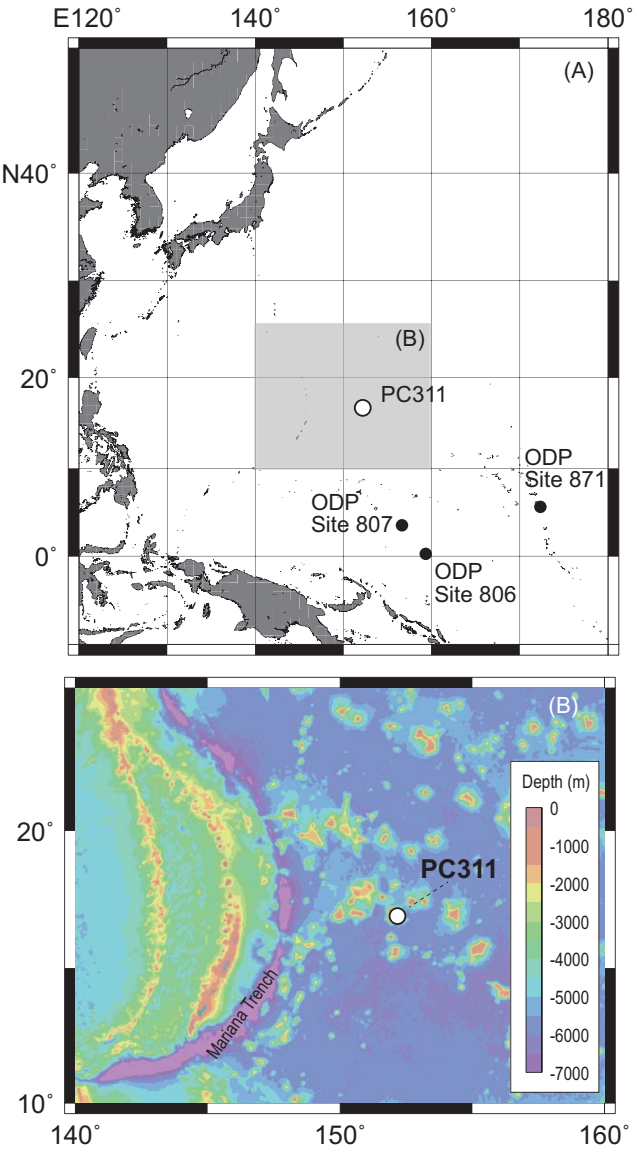

Figure 1. Location of core PC311 (**A** and **B**) in the Magellan Seamounts of the western Pacific Ocean.

Nomura (1995). Taxonomic assignments followed van Morkhoven *et al.* (1986), Jones (1994) and Kawagata (1999). The generic classification of Loeblich and Tappan (1987) was used and updated in certain instances, particularly for the uniserial taxa presented by Hayward *et al.* (2012) and for Cassidulinidae presented by Nomura (1983a, b, 1999).

We calculated the abundance of benthic foraminifera per unit weight of sediment using the specimen counts, number of splits, and weight of each sample. Expected diversity $E(S_n)$ (expected number of species in samples rarefied to n individuals; $n=50$) was calculated for each sample in the statistical programming environment R (R Development Core Team, 2020) using the function from the Vegan community ecology package (Oksanen *et al.*, 2019). The values of the Shannon-Wiener function (H') (this is the same as $H(S)$ in Buzas and Gibson [1969]) and the Buzas-Gibson evenness (originally equitability in Buzas and Gibson [1969]) were calculated using Microsoft Excel.

Planktonic foraminifera

Half of each washed residue aliquot from the 62 samples was used for the planktonic foraminiferal biostratigraphic study. Planktonic foraminiferal specimens larger than 125 μm were observed using a binocular microscope. A total of 10,000–40,000 specimens were observed for each sample.

In this study, the planktonic foraminiferal zonal scheme, biohorizons and taxonomy generally followed Wade *et al.* (2011; Supplementary document), who modified the zonal scheme of Berggren *et al.* (1995a, b) and compiled the astronomically tuned ages of planktonic foraminiferal biohorizons. In addition, the temporal changes of dominant coiling direction of *Pulleniatina* spp. have been used as a good stratigraphic marker for global correlation (Saito, 1976; Pearson and Penny, 2021). Pearson and Penny (2021) examined high-resolution coiling direction changes at IODP Sites U1483 and U1486 in the western tropical Pacific and the northwest Australian margin of the Indian Ocean, respectively. We referred to this framework as the reference succession of coiling direction change in this genus.

Calcareous nannoplankton

For the 44 samples in the lower part of core PC311 (598–235 cm), calcareous nannofossil analysis for age estimation was conducted at Palynosurvey Co. Ltd. Sediment samples were processed following Takayama (1978). A small amount of the dried sediment was placed in a small beaker and suspended in 20 ml of water. The suspension was placed in a plastic straw tube after mixing for approximately 30 seconds and then placed on a cover glass (18 mm×23 mm). The suspension was then dried on a hotplate at ~40°C before being mounted on a microslide using Norland Optical Adhesive.

Two hundred nannofossils were identified and counted under a binocular phase-contrast microscope with a polarizing unit. Taxonomic assignments followed those of Aubry (1984), Perch-Nielsen (1985), Pujos (1987), and Young (1998). The genus *Gephyrocapsa* was first identified at the species-level, and then other forms (i.e., *Gephyrocapsa* spp.) were assigned to large (>6 μm), medium (3–6 μm), and small (<3 μm) size groups based on the coccolith long diameter, following Takayama and

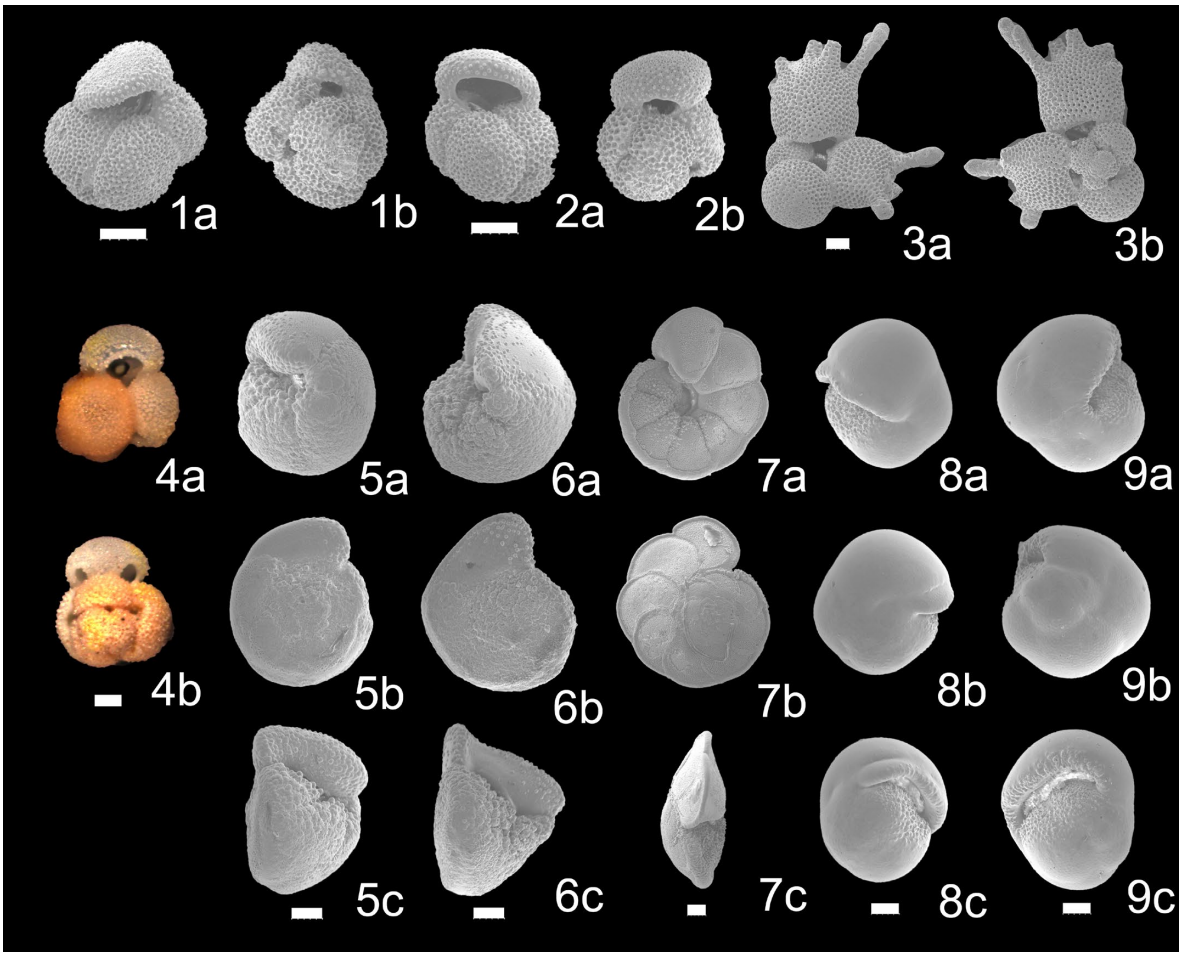

Figure 2. Scanning electron and light micrographs of selected planktonic foraminifera with sample horizons in core PC311. Scale bars are 100 µm. **1a, b,** *Globigerinoides obliquus* Bolli, 545.5 cm; **2a, b,** *Globigerinoides extremus* Bolli and Bermudez, 545.5 cm; **3a, b,** *Globigerinoidesella fistulosa* (Schubert), 545.5 cm; **4a, b,** *Globigerinoides ruber* (d'Orbigny) (pink form), 75.5 cm; **5a–c,** *Globorotalia truncatulinoides* (d'Orbigny), 75.5 cm; **6a–c,** *Globorotalia tosaensis* Takayanagi and Saito, 105.5 cm; **7a–c,** *Menardella multicamerata* (Cushman and Jarvis), 585.5 cm; **8a–c,** *Pulleniatina obliquiloculata* (Parker and Jones) (dextral from), 105.5 cm; **9a–c,** *Pulleniatina obliquiloculata* (Parker and Jones) (sinistral from), 105.5 cm. a: umbilical side, b: dorsal side, c: edge side.

Sato (1987) and Matsuoka and Okada (1989). Neogene calcareous nannofossil datums were adopted as proposed by Okada and Burkry (1980), Takayama and Sato (1987), Sato and Takayama (1992), and Sato *et al.* (1998). In addition, revised ages for datums from the Pleistocene and Pliocene were adopted from Sato *et al.* (2009).

Biostratigraphic age inference

A biohorizon may be present at any point between two samples. In addition, each sample is 1-cm thick. To account for this, we considered the sampling range for each data point, as we reported the depth of each biohorizon. For example, we recognized that the top horizon of a species lies between the base of the upper sample and the base of the lower sample. We converted these horizons into biostratigraphic ages based on *Geologic Time Scale 2020* (Neogene: Raffi *et al.*, 2020; Quaternary: Gibbard and Head, 2020). Within the disturbance interval (298–268 cm), we considered a datum with a 30-cm thickness to be within the error range.

Results and discussion

Biostratigraphic age inferences of core PC311

Planktonic foraminifera

Planktonic foraminifera were found in all 47 samples (Supplementary table 1). The preservation of foraminiferal tests was moderate to good (Figure 2). Figure 3 shows the stratigraphic occurrence of the index species in core PC311. The last occurrences of *Menardella mul-*

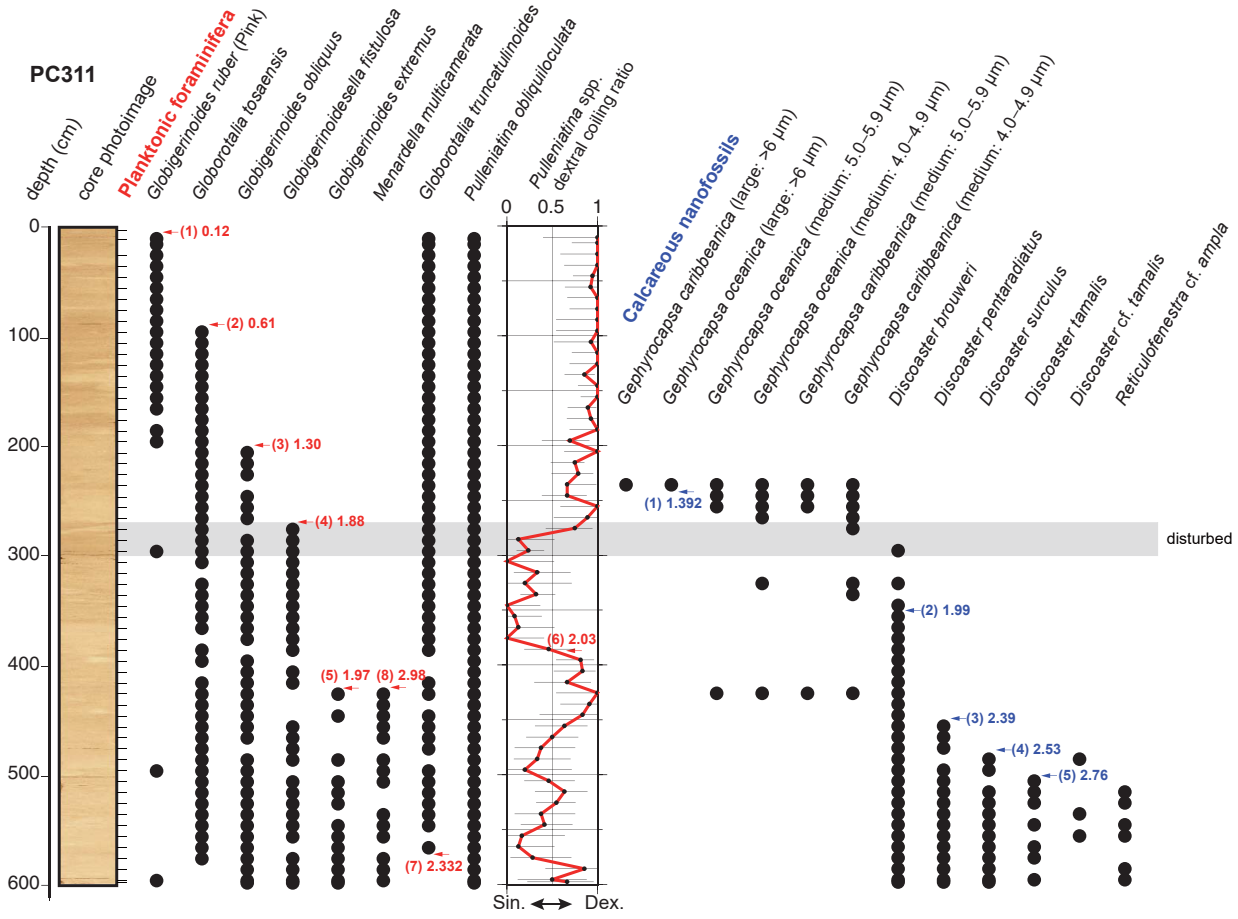

Figure 3. Stratigraphic occurrences of index taxa of planktonic foraminifera and calcareous nannofossils in core PC311. Gray shading shows the disturbed interval (298–268 cm). Datums are shown, as follows (FO: first occurrence; LO last occurrence). Planktonic foraminifera: (1) LO *Globigerinoides ruber* (pink from) (0.12 Ma); (2) LO *Globorotalia tosaensis* (0.61 Ma); (3) Top *Globigerinoides obliquus* (1.30 Ma); (4) LO *Globigerinoidessella fistulosa* (1.88 Ma); (5) LO *Globigerinoides extremus* (1.97 Ma); (6) Base of W4 of dextral coiling ratio of *Pulleniatina* (2.03 Ma) with 95% confidence interval; (7) FO *Globorotalia truncatulinoides* (2.332 Ma); (8) LO Menardella multicamerata (2.98 Ma). Calcareous nannofossils: (1) FO *Gephyrocapsa* (large) (1.392 Ma); (2) LO *Discoaster brouweri* (1.99 Ma); (3) LO *Discoaster pentaradiatus* (2.39 Ma); (4) LO *Discoaster surculus* (2.53 Ma); (5) LO *Discoaster tamalis* (2.76 Ma). Sin.: sinistral coiling, Dex.: dextral coiling.

ticamerata and *Globigerinoides extremus*, *Globigerinoidesella fistulosa*, *Globigerinoides obliquus*, *Globorotalia tosaensis* and *Globigerinoides ruber* (pink form) were observed at 420.5 cm, 270.5 cm, 200.5 cm, 90.5 cm and 6.5 cm, respectively (Figure 3). On the other hand, the first occurrence of *Globorotalia truncatulinoides* was recognized at 570.5 cm (Figure 3). In addition, a change from dextral to sinistral coiling direction in *Pulleniatina* is observed at 380.5 cm (Figure 3), corresponding to W4 in Pearson and Penny (2021).

Based on the above results, the following datums for planktonic foraminifera are inferred. The first occurrence of *G. truncatulinoides* at 2.332 Ma was observed at 570.5 cm. The first appearance of this species is usually constrained to 1.93 Ma, whereas a diachrony on the first appearance of this species at 2.332 Ma was reported at ODP Site 806 (e.g. Lam *et al.*, 2022). In the present study, we adopted the first appearance of this species as recognized by Lam *et al.* (2022). In addition, the last occurrences of *G. obliquus* (1.30 Ma), *G. tosaensis* (0.61 Ma) and *G. ruber* (pink form) (0.12 Ma) were observed at 200.5 cm, 90.5 cm and 6.5 cm, respectively. The last occurrence of *G. fistulosa* (1.88 Ma) was also observed at 270.5 cm, although we adopted this as the reference datum within the error range due to the core disturbance (298–268 cm). Furthermore, a change in the coiling direction of *Pulleniatina* at 2.03 Ma (Pearson and Penny, 2021) was observed at 385.5 cm (Supplementary figure 2). However, we judged that the last occurrence of *M. multicamerata* (2.98 Ma) at 420.5 cm was reworked com-

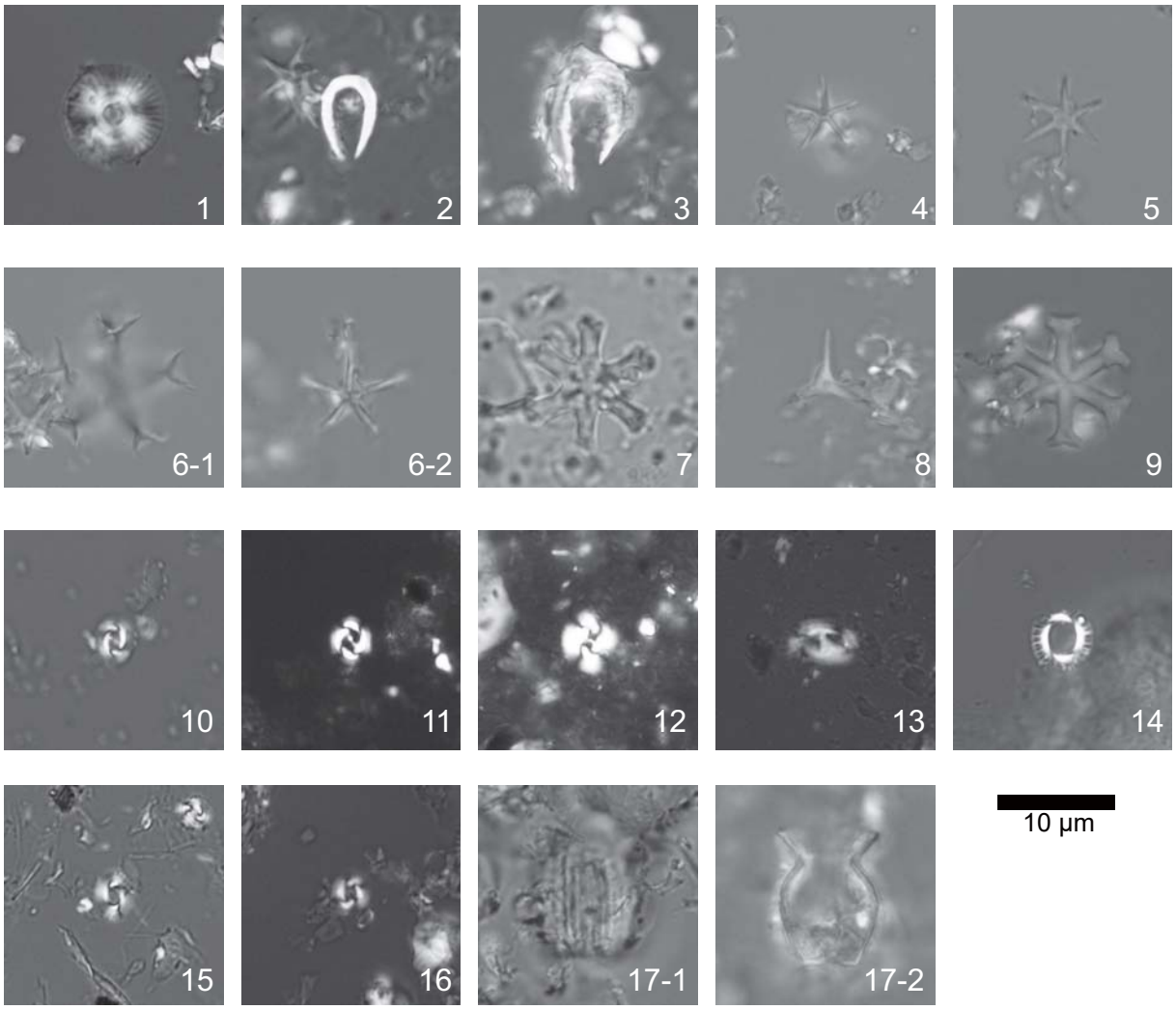

Figure 4. Light micrographs (polarizing microscope images) of selected calcareous nannofossils with sample horizons from core PC311. Scale bar is 10 μm. **1,** *Calcidiscus macintyrei* (Bukry and Bramlette) Loeblich and Tappan, 245.5 cm; **2,** *Ceratolithus cristatus* Kamptne, 265.5 cm; **3,** *Ceratolithus rugosus* Bukry and Bramlette, 385.5 cm; **4,** *Discoaster asymmetricus* Gartner, 425.5 cm; **5,** *Discoaster brouweri* Tan Sin Hok, 355.5 cm; **6-1,** *Discoaster pentaradiatus* Tan Sin Hok, 455.5 cm; **6-2,** *Discoaster pentaradiatus* Tan Sin Hok, 455.5 cm; **7,** *Discoaster surculus* Martini and Bramlette, 535.5 cm; **8,** *Discoaster triradiatus* Tan Sin Hok, 355.5 cm; **9,** *Discoaster variabilis* Martini and Bramlette, 535.5 cm; **10**, *Gephyrocapsa oceanica* Kamptner, 255.5 cm; **11,** *Gephyrocapsa caribbeanica* Boudreaux and Hay, 265.5 cm; **12,** *Gephyrocapsa* spp. (large: >6 μm), 235.5 cm; **13,** *Helicosphaera sellii* Bukry and Bramlette, 345.5 cm; **14,** *Pseudoemiliania lacunose* (Kamptner) Gartner, 275.5 cm; **15,** *Reticulofenestra* cf. *ampla* Sato, Kameo and Takayama, 595.5 cm; **16,** *Reticulofenestra minutula* (Gartner, 1967) Haq and Berggren, 525.5 cm; **17-1,** *Scyphosphaera pulcherrima* Deflandre, 425.5 cm; **17-2,** *Scyphosphaera pulcherrima* Deflandre, 425.5 cm.

pared with the other datums. In addition, the last occurrence of *G. extremus* (1.97 Ma) at 420.5 cm appeared less reliable than the stratigraphic position of W4 for the coiling direction of *Pulleniatina*.

Calcareous nannoplankton

Calcareous nannofossils were found in all 44 samples from the lower to middle part (597.5–230.5 cm) of core PC311 (Supplementary table 2). The preservation was generally moderate to good (Figure 4). Figure 3 shows the stratigraphic occurrences of the index species in core PC311. The last occurrences of *Reticulofenestra* cf. *ampla*, *Discoaster tamalis*, *Discoaster surculus*, *Discoaster pentaradiatus* and *Discoaster brouweri* were observed at 510.5 cm, 500.5 cm, 480.5 cm, 450.5 cm and 350.5 cm, respectively (Figure 3). On the other hand, the first occurrences of *Gephyrocapsa caribbeanica*, *Gephyrocapsa oceanica* and *Gephyrocapsa* (large) were observed at 270.5 cm, 260.5 cm and 240.5 cm, respectively (Figure 3).

From the above results, the datums for calcareous nannofossils are inferred as follows: The last occurrences of *D. tamalis* (2.76 Ma), *D. surculus* (2.53 Ma) and *D. pentaradiatus* (2.39 Ma) were observed at 500.5 cm, 480.5 cm and 450.5 cm, respectively. Although the last occurrence of *D. brouweri* at 1.99 Ma was difficult to specify owing to sporadic upward occurrences, we observed the last occurrence at 350.5 cm, based on its end of continuous occurrence. Determining the stratigraphic positions of the first occurrences of *G. caribbeanica* (1.763 Ma) and *G. oceanica* (1.706 Ma) was also problematic because of their continuous but sporadic occurrences. Thus, we do not recognize these datums, mainly because of core disturbance interval (298–268 cm). The first occurrence of *Gyphyrocapsa* (large) at 1.392 Ma was observed at 240.5 cm.

The last occurrence of *D. brouweri* and the first appearances of *G. caribbeanica* and *G. oceanica* were un clear (Figure 3). The unusual occurrences of these calcareous nannofossils in the core disturbance interval (298–268 cm) may represent possible contamination, and we excluded these datums from the discussion of age inferences.

Age models and sedimentation rate

Figure 5 shows the age-depth relationship based on the stratigraphic horizons of the datums of planktonic foraminifera and calcareous nannofossils in core PC311. Compared to the stratigraphic horizons of the datums, several differences were observed between the two fossil groups. Planktonic foraminifera showed a relatively younger age at 575 cm, whereas the calcareous nannofossils showed relatively older ages in the lower part of the core (Figure 5A; Supplementary table 3).

We used the coiling direction of *Pulleniatina* in core PC311 as an independent time marker (Figure 3). The first occurrence of *Gephyrocapsa* (large) was consistent with this marker, whereas the last occurrences of *D. pentaradiatus* and *D. surculus* were inconsistent with it. However, because the coiling direction of *Pulleniatina* was not uniform between IODP Sites U1483 (Timor Sea) and U1486 (Bismark Sea) (Pearson and Penny, 2021), it was difficult to evaluate whether the last occurrence of *D. tamalis* was reliable or not using this metric. Therefore, the last occurrences of *D. pentaradiatus* and *D. surculus* were dismissed as unreliable datums, because of possible reworking. Instead, we used the first occurrence of *Gephyrocapsa* (large) and the last occurrence of *D. tamalis*.

We attempted to construct two age models based on the biostratigraphic datums of both planktonic foraminifera and calcareous nannofossils because these two fossil groups differ slightly in their stratigraphic positions in the

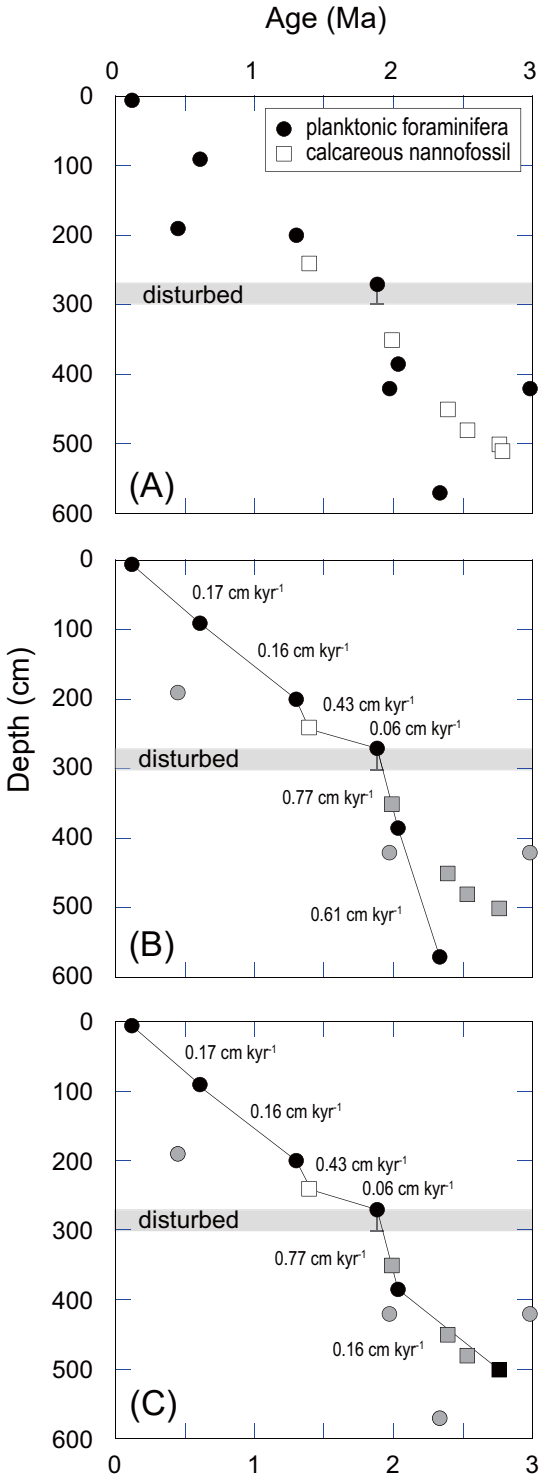

Figure 5. Age-depth plots of core PC311. All the datums in this study (**A**); the selected datums for first and second age models (**B, C**), respectively. Gray-symbols in panels (B) and (C) represent the excluded datums for the age inferences. Gray shading shows the disturbed interval (298–268 cm). In addition, the datum at 271 cm is shown with an error range (298–268 cm).

lower part of the core (Figure 5B, C). The first age model adopts the first occurrence of *G. truncatulinoides* (2.332 Ma) at 570.5 cm as the core bottom age (Figure 5B). The second age model adopted the last appearance of *D. tamalis* (2.76 Ma) at 500.5 cm (Figure 5C). Based on the comparison of the coiling ratio of *Pulleniatina* and the faunal association of planktonic foraminiferal fauna, the first age model seems more plausible with less influence by the possible reworking of microfossils. In contrast, Khim *et al.* (2025) recently implied a possible diachrony for the first occurrence of *G. truncatulinoides* in core WP-GPC-202302, which was collected near PC311 core site. Thus, both age models should be argued further using additional datums compared to other age determinations in the surrounding areas.

According to the first age model, sedimentation rates were higher in the lower part of the core (0.06–0.76 cm kyr^{-1} below ~270 cm) than in the upper part (0.17–0.43 cm kyr^{-1} above ~270 cm) (Figure 5B). Because the study site moved in the WNW direction with the Pacific Plate motion, the sedimentation rate change might be partially attributed to the tectonic movement of the study site. Given that the Pacific Plate moves by ~8 cm yr^{-1}, the position of the core site drifted by ~152 km between ~1.9 Ma (~270 cm) and the present day. Therefore, it is difficult to consider that the core site has experienced the different water mass or different climatic zone of the present day due to the plate motion.

Several studies have suggested that the mean position of the ITCZ has migrated southward in the equatorial Pacific Ocean since the MPT (e.g. Seo *et al.*, 2015; Wang *et al.*, 2023). In particular, Wang *et al.* (2023) suggested that surface water salinity decreased from ~1.8 to 0.5 Ma based on the oxygen isotope record of seawater at ODP Site 871 (5.56°N) (Supplementary figure 3). They interpreted the cause of the long-term decline in surface water salinity to be increasing precipitation at ODP Site 871 due to the southward ITCZ displacement. Because the present-day collection site (~17°N) of core PC311 is located at the boundary (more oligotrophic) between the NEC and the NPG, the southward movement of the mean ITCZ position may affect the decrease of primary production. Because core PC311 primarily consists of biogenic carbonates such as calcareous nannofossils and foraminifera, the decreasing sedimentation rate above ~270 cm (~1.9 Ma) may be explained by the southward displacement of the mean ITCZ position, migrating from the equatorial wind-driven mixing zone, which is characterized by relatively high primary production.

Faunal associations of Quaternary benthic foraminifera in core PC311

Structure of the community and faunal association

Fossil benthic foraminifera were observed in all 32 samples from core PC311 (Supplementary table 4). There was no apparent destruction or abrasion of tests of benthic foraminifera, even in taxa with fragile and thin test walls such as *Epistominella exigua* and *Alabaminella weddellensis* (Figures 6–8). Although we cannot solely dismiss possible transportation of the foraminiferal tests, these observations suggest that the benthic foraminiferal fauna was unlikely to be disturbed by strong transportation from other areas to the core site. The test conditions of benthic foraminifera also suggested no marked dissolution effect on the faunal data. In fact, because the %coarse fraction (>63 μm) is regarded as a proxy of carbonate corrosivity on the seafloor, it is generally stable throughout the core except for the lowermost part (Figure 9). This observation supports the absence of a marked change in carbonate corrosivity throughout core PC311.

The abundance of benthic foraminifera (i.e., number of occurrences per gram of sediment), ranging between 160 and 1421 individuals per unit weight (Figure 9), was high in the interval above 200 cm with frequent fluctuations compared to the interval below 200 cm. This pattern is generally similar to that of the %coarse fraction (Figure 9). *Globocassidulina subglobosa*, *Globocassidulina obtusa*, *Pullenia* spp. and *Cibicidoides mundulus* were common constituents, subordinated with *Paracassidulina sulcata*, *E. exigua*, *A. weddellensis*, *Oridorsalis umbonatus*, *Gyroidinoides* sp. A and *Astrononion echolsi* (Figures 6–10). It can be difficult to differentiate between *Globocassidulina subglobosa* and *Globocassidulina ryukyuensis* (Figure 6) in younger individuals because of their similar test morphologies. In this study, we regarded these two species as a combination, *Globocassidulina subglobosa–Globocassidulina ryukyuensis* plexus. Both rarefaction ($E[S_{50}]$) and Shannon-Wiener (H') are high in the interval below ~220 cm, particularly in ~570–540 cm (Figure 9). In contrast, both species diversity measures were relatively low above 200 cm, with a large temporal decline at 60 cm. Evenness of Buzas and Gibson (1969) decreased significantly in the interval above ~200 cm, which was close to the beginning of the relatively low species diversity indices ($E[S_{50}]$ and Shannon-Wiener [H']). These decreasing patterns in the community structure across ~200 cm were generally the opposite of the increasing pattern in the abundance of benthic foraminifera (Figure 9).

Stilostomellidae and Pleurostomellidae generally decreased upward, with several fluctuations in the interval above ~200 cm (Figure 10) and disappeared at ~60 cm.

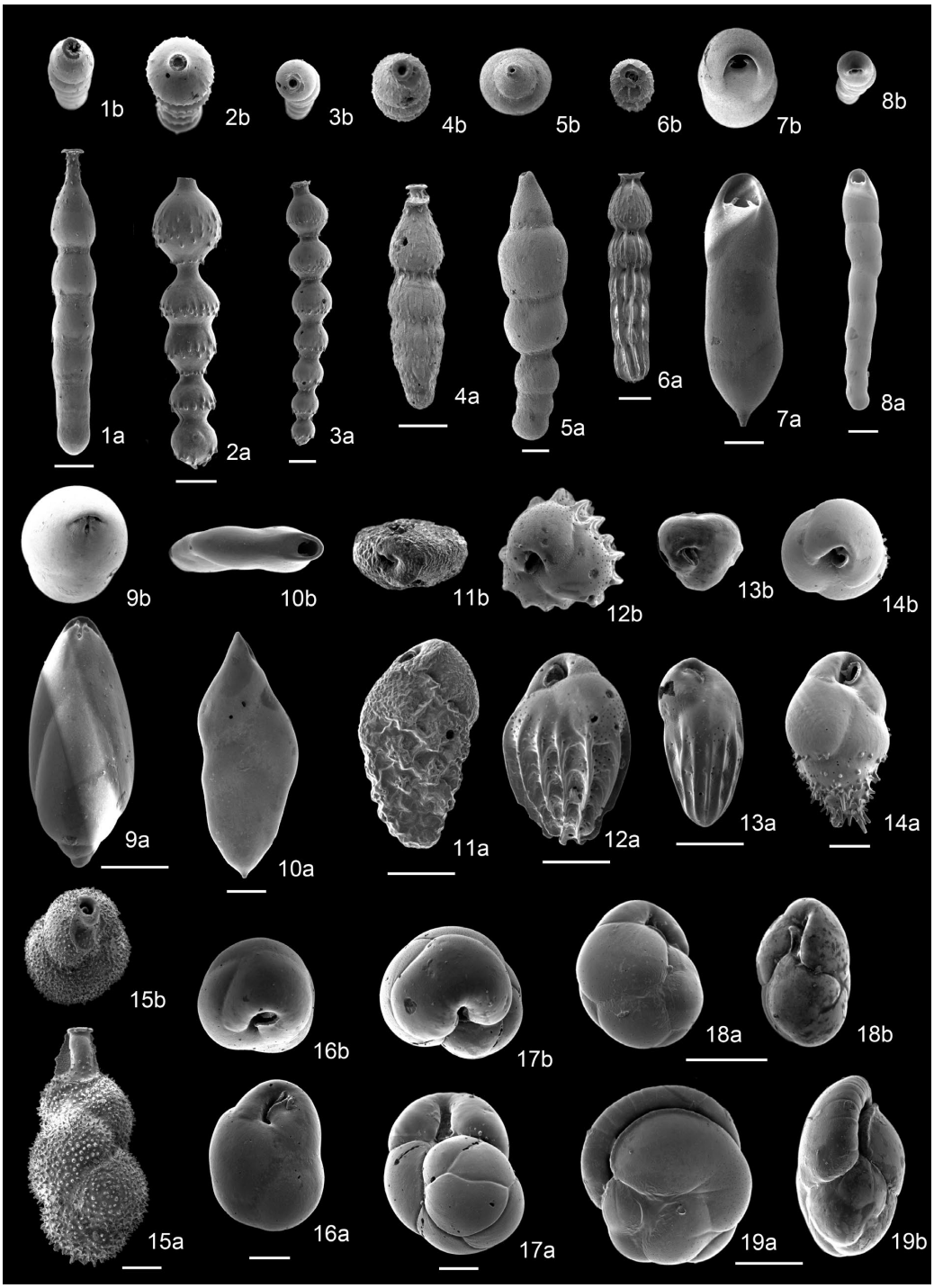

Figure 6. Scanning electron micrographs of selected benthic foraminifera with sample horizons from core PC311. Scale bars are 100 μm. **1a, b,** *Strictocostella hyugaensis* (Ishizaki), 225.5 cm; **2a, b,** *Siphonodosaria jacksonensis* (Cushman and Applin), 165.5 cm; **3a, b,** *Siphonodosaria jacksonensis* (Cushman and Applin) sensu Hayward *et al*. (2012), 305.5 cm; **4a, b,** *Strictocostella spinata* (Cushman), 385.5 cm; **5a, b,** *Orthomorpina jedlitschkai* (Thalmann), 597.5 cm, **6a, b,** *Strictocostella modesta* (Bermudez), 597.5 cm; **7a, b,** *Pleurostomella acuta* Hantken, 545.5 cm; **8a, b,** *Pleurostomella subnodos*a (Reuss, 1851), 545.5 cm; **9a, b,** *Obesopleurostomella parviapertura* (Kennett), 225.5 cm; **10a, b,** *Pleurostomella lata* Keyzer, 225.5 cm; **11a, b,** *Abditodentrix pseudothalmanni* Boltovskoy and Guissani de Kahn, 125.5 cm; **12a, b,** *Bulimina rostratiformis* McCulloch, 345.5 cm; **13a, b,** *Bulimina truncana* Gümbel, 145.5 cm; **14a, b,** *Bulimina aculeata* d'Orbigny, 10.5 cm; **15a, b,** *Uvigerina proboscidea* Schwager, 245.5 cm; **16a, b,** *Globocassidulina ryukyuensis* Nomura, 485.5 cm; **17a, b,** *Globocassidulina subglobosa* (Brady), 185.5 cm; **18a, b,** *Globocassidulina obtusa* (Williamson), 185.5 cm; **19a, b,** *Paracassidulina sulcata* (Belford), 405.5 cm.

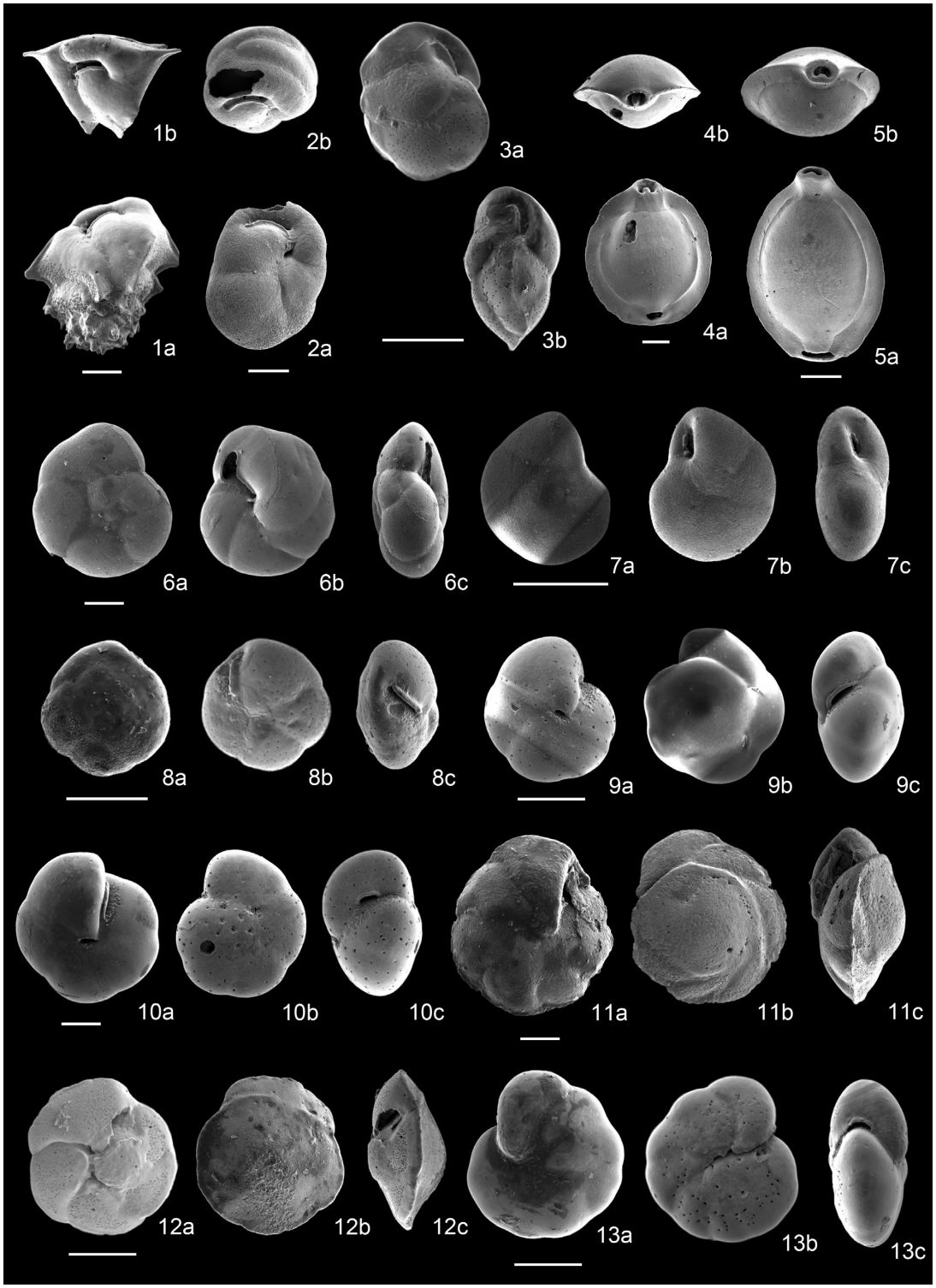

Figure 7. Scanning electron micrographs of selected benthic foraminifera with sample horizons from core PC311. Scale bars are 100 µm. **1a, b,** *Ehrenbergina trigona* Goës, 465.5 cm; **2a, b,** *Burseolina* sp., 10.5 cm; **3a, b,** *Globocassidulina lenticularis* Nomura, 185.5 cm; **4a, b,** *Pyrgo murrhina* (Schwager), 10.5 cm; **5a, b,** *Pyrgo* cf. *murrhina* (Schwager), 65.5 cm; **6a–c,** *Pseudoparrella obtus*a (Burrows and Holland), 65.5 cm; **7a–c,** *Epistominella exigua* (Brady), 185.5 cm; **8a–c,** *Alabaminella weddellensis* Earland, 125.5 cm; **9a–c,** *Oridorsalis umbonatus* (Reuss), 45.5 cm; **10a–c,** *Gyroidinoides* sp., 265.5 cm.; **11a–c,** *Osangularia culter* (Parker and Jones), 185.5 cm; **12a–c,** *Gavelinopsis praegeri* (Heron-Allen and Earland), 185.5 cm; **13a–c,** *Cibicidoides mundulus* (Brady *et al.*), 265.5 cm.

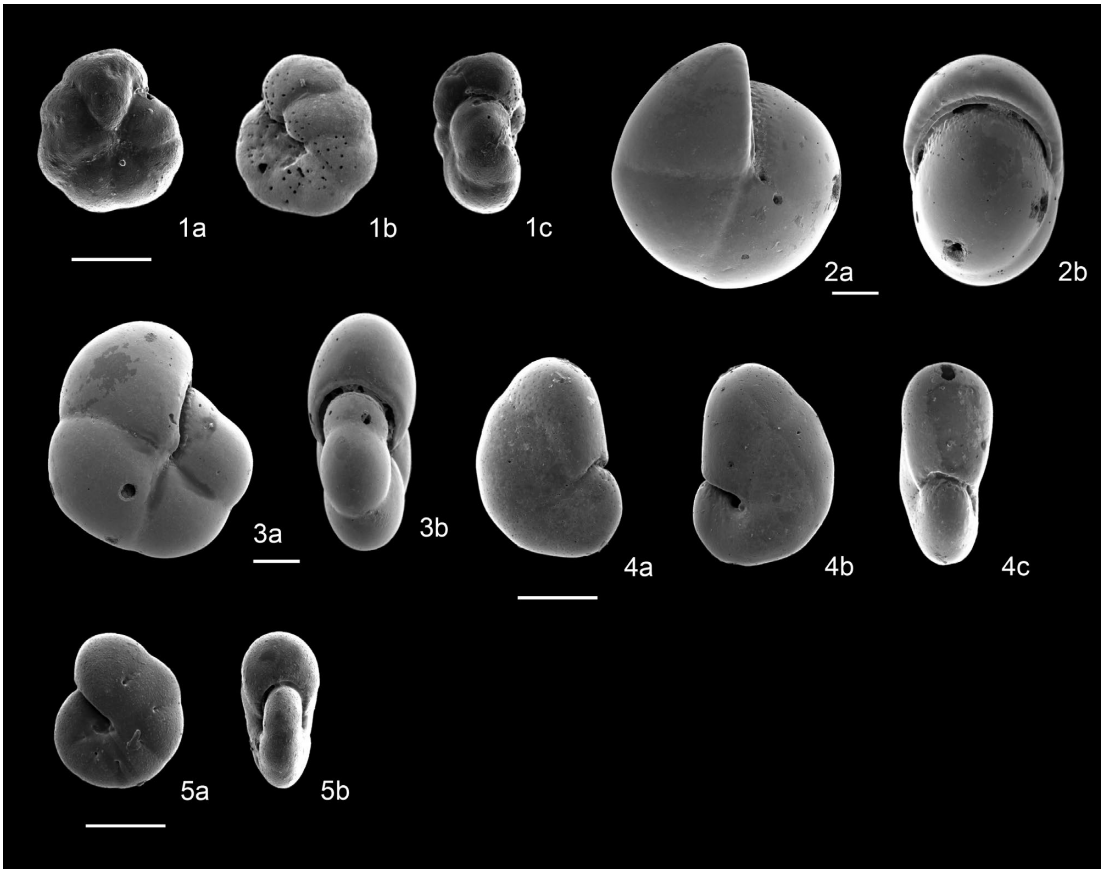

Figure 8. Scanning electron micrographs of selected benthic foraminifera with sample horizons from core PC311. Scale bars are 100 µm. **1a–c,** *Hetrolepa dutemplei* (d'Orbigny), 265.5 cm; **2a, b,** *Pullenia bulloides* (d'Orbigny), 165.5 cm; **3a, b,** *Pullenia salisburyi* Stewart and Stewart, 165.5 cm; **4a–c,** *Pseudononion* sp. A, 265.5 cm; **5a, b,** *Astrononion echolsi* Kennett, 265.5 cm.

These taxa became extinct across the MPT (e.g. Hayward *et al.*, 2010, 2012). Our results also imply the extinction of these taxa across the Early/Middle Pleistocene, which is similar to the results of previous studies (e.g. Hayward *et al.*, 2012). These extinct taxa may explain the general decreasing trend in species diversity in the upper part of the core (Figures 9, 11). Alternatively, *Abditodentrix pseudothalmanni* increased throughout the 200–100 cm interval (Figure 10). In addition, Stilostomellidae temporally decreased between ~380–200 cm (centered at approximately 300 cm), whereas *A. echolsi* temporally increased throughout this interval. Thus, the faunal transition of benthic foraminifera was observed at ~200 cm and temporally at ~60 cm in core PC311, based on the diversity measures (Figure 9). In addition, temporal and gradual changes in the faunal association occurred in ~380–200 cm (centered at ~300 cm) (Figure 11).

Over ~2 million years, an increase of *A. echolsi* with a temporal decrease of Stilostomellidae was discernible in the middle part of the core (~380 cm and 200 cm). Because *A. echolsi* seems to be a species related to the Southern Ocean-originated deep water (Nomura, 1995), the common occurrence of *A. echolsi* may be explained by the greater influence of the Southern Ocean-originated deep water (i.e., UCDW in the Pacific Ocean) at the shallower (lower bathyal) depth of our study site. Although the formation of the NPDW intensified during the Early Pliocene, it gradually weakened over time (e.g. Burls *et al.*, 2017). The neodymium isotope of bulk carbonates and carbon stable isotope data of benthic foraminifera from ODP Site 807 (2807 m water depth at present) imply a gradual weakening of NPDW formation toward ~2 Ma (Figure 11; Le Houedec *et al.*, 2016; Feng *et al.*, 2022). The termination of the NPDW formation and the greater influence of the UCDW on our study site may have affected the faunal changes of benthic foraminifera in core PC311 at the lower bathyal depth of the western Pacific Ocean.

Deep-sea benthic foraminifera in pelagic settings are thought to strongly depend on the food supply from the

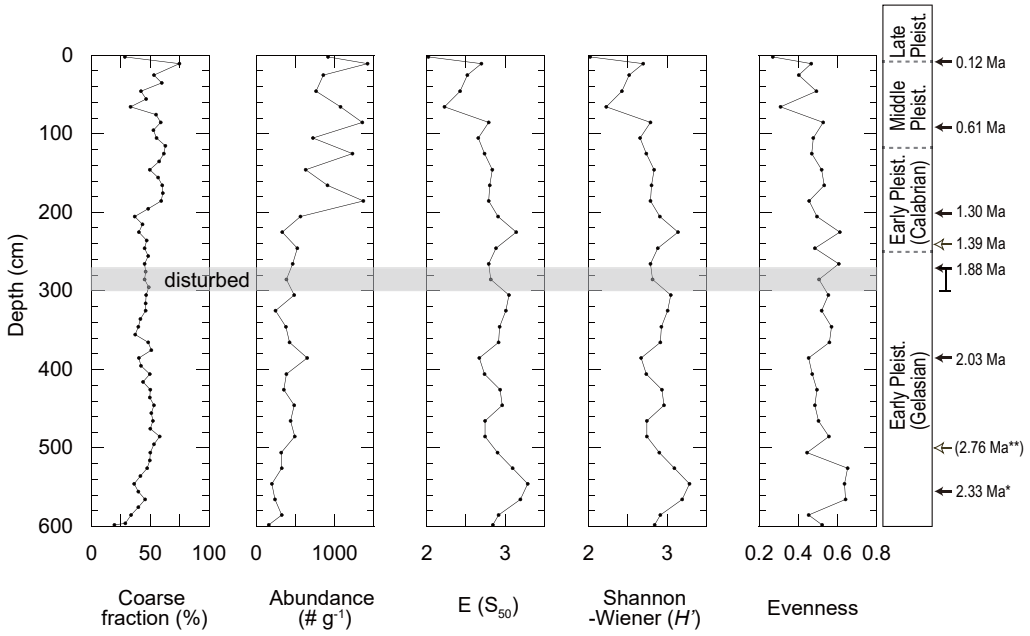

Figure 9. Stratigraphic variations of the %coarse fraction, abundance of benthic foraminifera per unit weight, and the species diversity measures (rarefaction ($E[S_{50}]$), Shannon-Wiener (H') and the evenness) of benthic foraminifera in core PC311. Gray shading shows the disturbed interval (298–268 cm). The age with parenthesis is supplementary calcareous nannofossil age.

ocean surface and various species adopt different trophic conditions (Gooday, 1994; Jorissen *et al.*, 2007). The relative abundance of *C. mundulus*, an oligotrophic species (e.g. Altenbach *et al.*, 1999), increased above ~180 cm (Figure 10). This is consistent with our interpretation of decreasing primary production in the upper part of the core presumably due to the southward migration of the mean ITCZ position, similar to the decreasing sedimentation rate. Although the abundance of benthic foraminifera per unit weight increased in the same interval, this can be interpreted by the expense of the decreasing matrix (i.e., fine fraction, such as calcareous nannoplankton).

Epistominella exigua was continuously common in the interval below ~180 cm, whereas *A. weddellenesis* increased in ~180–70 cm and *Pseudoparrella obtusa* was occasionally dominant in the interval above ~180 cm, particularly at ~70 cm and the core-top (Figure 10). *Epistominella exigua* and *A. weddellensis* are phytodetritus species that can adapt to an episodic food supply from the ocean surface (e.g. Gooday, 2003). Although there is little ecological information on *P. obtusa*, the test morphology of this species is similar to that of the phytodetritus species, which is characterized by the small test and thin walls with relatively large comma-shaped apertures with teeth (Figure 7). These alternations in common taxa could be explained by the replacement of ecological niches after major extinction across the MPT.

Throughout the Quaternary, SST in the western Equatorial Pacific Ocean has changed little, whereas SST in the eastern Equatorial Pacific Ocean has declined since the Pliocene owing to the enhancement of equatorial upwelling by trade winds (e.g. Fedorov *et al.*, 2015). The faunal transitions in core PC311 at ~1.3 Ma was roughly coincident with the enhancement on the zonal SST gradient between the eastern and western Equatorial Pacific Ocean (e.g. Fedorov *et al.*, 2015; Figure 11). The enhanced zonal SST gradient may stimulate interannual variations in food supply from surface water in the Equatorial Pacific Ocean (e.g. Fedorov *et al.*, 2015). Consequently, such an enhanced interannual variation in food supply may explain the increased episodic food supply from the ocean surface to the benthic foraminiferal fauna on the seafloor.

In summary, the faunal transition of bathyal benthic foraminifera in core PC311 can be attributed to changes in deep-water circulation, including the influence of the NPDW/UCDW and the enhancement of the zonal SST gradient between the eastern and western Equatorial Pacific Oceans. These paleoceanographic circumstances may also provide important clues for understanding the long-term transition of present-day deep-sea benthic foraminifera in the low-latitude pelagic region of the western Pacific Ocean.

Diversification of Cassidulinidae during the Quaternary

Another feature of the benthic foraminiferal faunas in

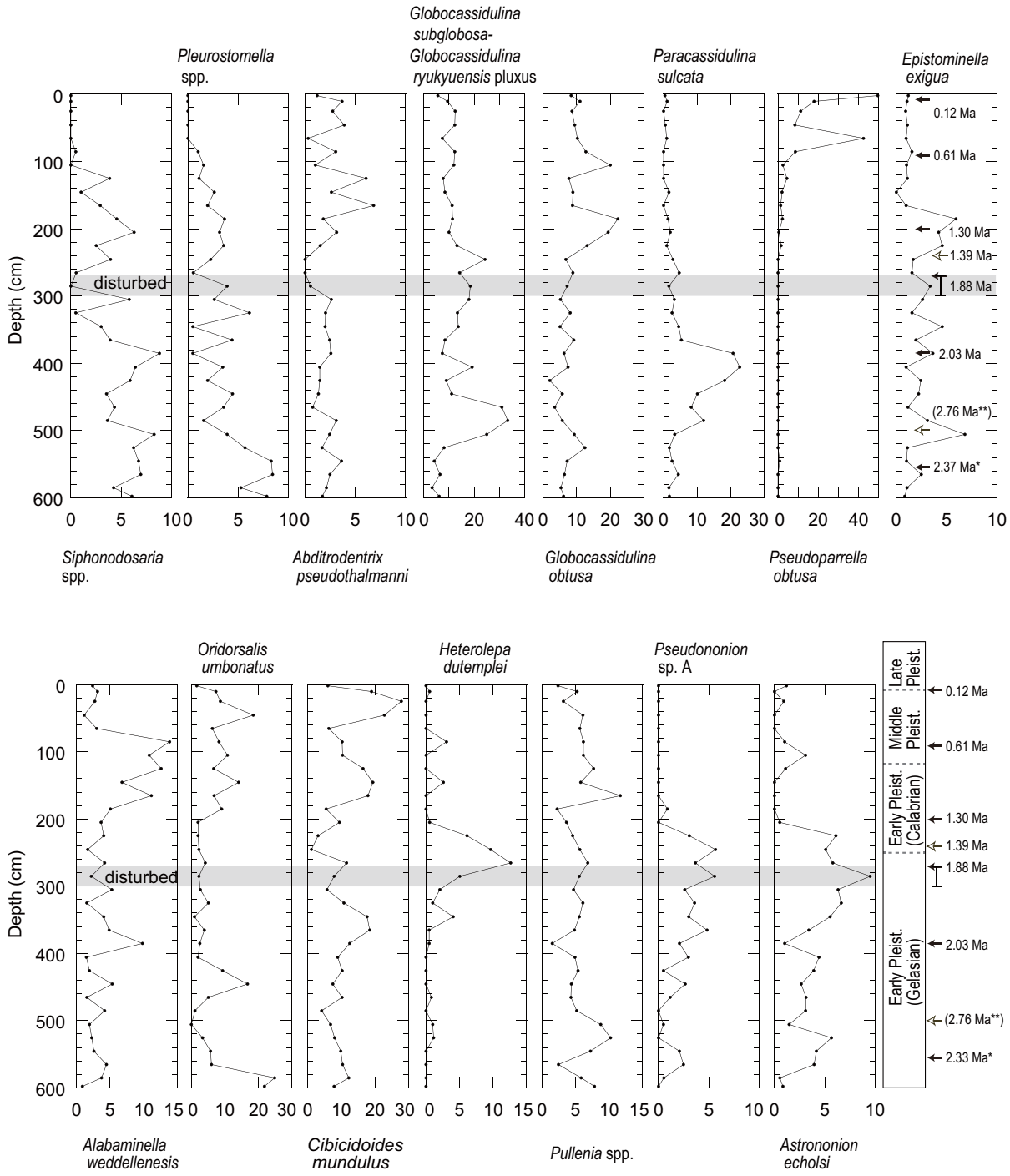

Figure 10. Stratigraphic variation (relative abundance) of selected major taxa of benthic foraminifera in core PC311. Gray shading shows the disturbed interval (298–268 cm). The age with parenthesis is supplementary calcareous nannofossil age.

core PC311 is the common occurrence of various species of Cassidulinidae beginning at ~2.4 Ma or ~2.8 Ma, depending on the first and second age models (Figure 5B, C). First, the *Globocassidulina subglobosa–Globocassidulina ryukyuensis* plexus was abundant in ~500–460 cm (~2.2 Ma or ~2.8–2.5 Ma based on the first or second age model). Then, *Paracassiduline sulcata* was abundant in ~460–380 cm (~2.0 Ma or ~2.2 Ma in the first or second

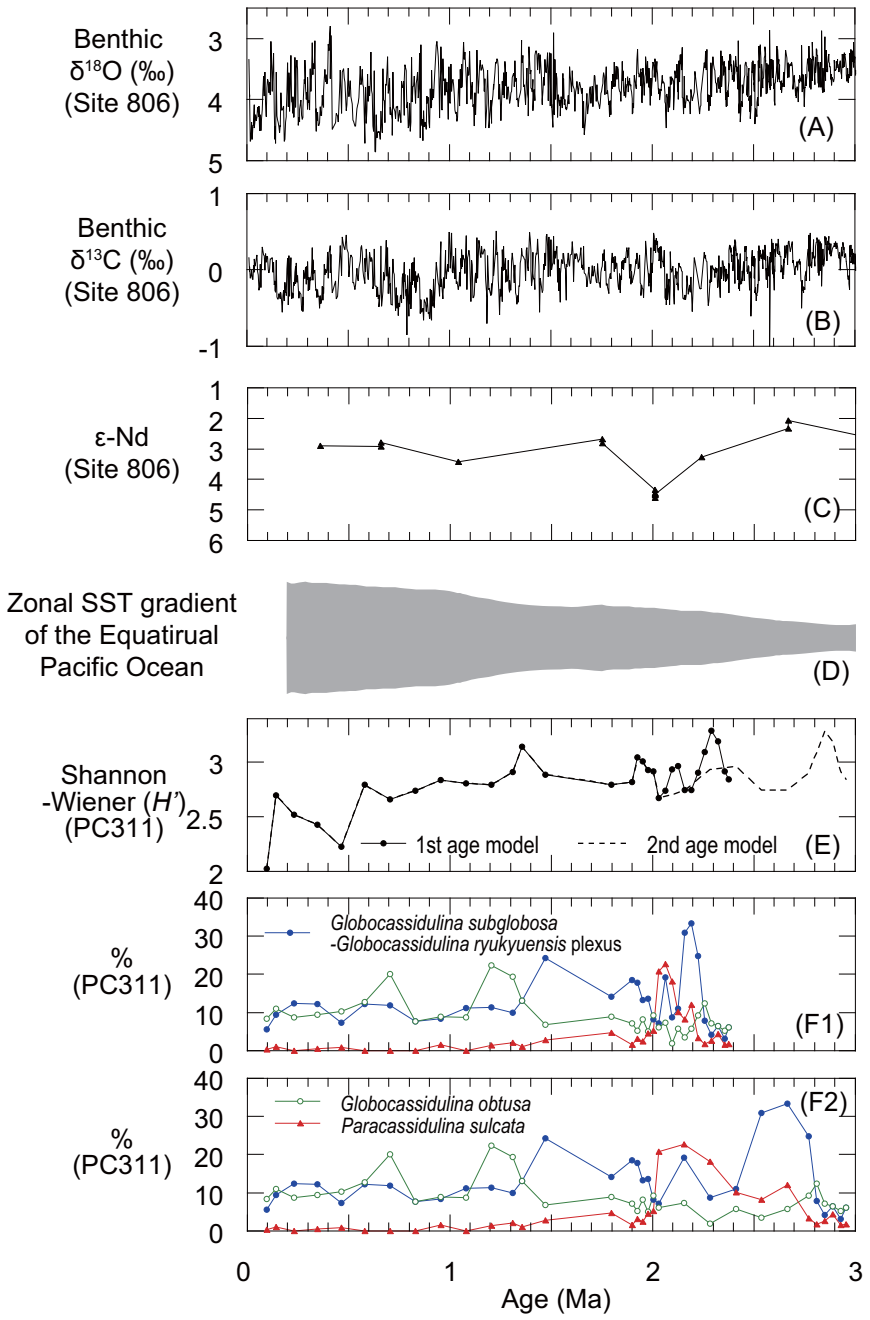

Figure 11. Time-series changes of oxygen and carbon stable isotope data of benthic foraminifera at ODP Site 807 (Feng *et al.*, 2022) (**A and B**), neodymium isotope (ε_{Nd}) of carbonate fraction at ODP Site 807 (Le Houedec *et al.*, 2016) (**C**), zonal sea-surface temperature (SST) gradient between the eastern and western Pacific Ocean (Fedorov *et al.*, 2015) (**D**), Shannon-Wiener (*H'*) of benthic foraminiferal fauna in core PC311 (**E**), and relative abundances of *Globocassidulina subglobosa–Globocassidulina ryukyuensis* plexus, *Globocassidulina obtusa* and *Paracassidulina sulcata* (**F1 and F2**) in core PC311. Panels (F1) and (F2) contain the same data, based on the first and second age models, respectively.

age model). Finally, *Globocassidulina obtusa* was common in the interval of ~220–180 cm (~1.4–1.1 Ma) and temporally at ~100 cm (Figure 11). The Pliocene–Pleistocene was a time of diversification for Cassidulinidae (Nomura, 1983b). The onset of the abundance of the *G. subglobosa–G. ryukyuensis* plexus with common *P. sulcata* from either ~2.4 Ma or ~2.8 Ma corresponds to the timing slightly after the NHG (Figure 11). In the North

Pacific Ocean, the transient formation of the NPDW weakened after the Early Pliocene (Figure 11; Le Houedec *et al.*, 2016; Feng *et al.*, 2022). Thus, the occurrence of Cassidulinidae appears to be related to deep-water circulation changes in the North Pacific Ocean.

In addition, *G. subglobosa* prefers deep-sea environments with high organic carbon content (Miao and Thunnel, 1993) or more pronounced seasonal food pulse (Gooday, 1994; Suhr *et al.*, 2003; Eberwein and Mackensen, 2006; Suhr and Pond, 2006; Gooday *et al.*, 2008). There are few ecological reports on *G. obtusa*, but this species seems to be recognized in other studies as *Globocassidulina crassa*. *Globocassidulina crassa* has been reported from bathyal depths in the Ross Sea, where its habitat is shallower than that of *G. subglobosa* (e.g. Fillon, 1974). Such an occurrence is consistent with our inference regarding the possible influence of the UCDW in ~380–200 cm, if the Southern Ocean-originated deep water continuously influenced at our study site. *Globocassidulina crassa* also responds to seasonal phytoplankton blooms (Suhr and Pond, 2006). Gastaldello *et al*. (2024) regarded this species as one of "phytodetritus exploiting taxa", with *G. subglobosa* in the western Equatorial Pacific Ocean. Given that *G. obtusa* as sampled from core PC311 has ecological characteristics similar to those of *G. crassa*, the common occurrence of *G. obtusa* is consistent with an intensified episodic food supply and an enhanced zonal SST gradient in the Equatorial Pacific Ocean (Figure 11). Thus, the diversification of Cassidulinidae in the lower bathyal zone of the low-latitude region of the western Pacific Ocean during the Early Pleistocene seems to have been affected by trophic changes, particularly the enhanced episodic food supply from the surface ocean in addition to the influence of the UCDW from the Southern Ocean-originated deep water.

Conclusions

We studied fossil calcareous nannoplankton and planktonic and benthic foraminifera during the Quaternary in core PC311 from the seamount top of the Magellan Seamounts (western Pacific Ocean). Our conclusions are as follows.

(1) Six and five datums were recognized by planktonic foraminifera and calcareous nannofossils, respectively. In the lower part of the core, a planktonic foraminiferal datum occurred at 2.332 Ma at 570.5 cm, whereas two datums of calcareous nannofossils were determined at 2.76 Ma at 500.5 cm. Based on these datums, we proposed two age models that differ below ~400 cm. The first age model is consistent with the coiling direction of *Pulleniatina* and the faunal association of planktonic foraminifera, although a precise age model should be evaluated further using more robust datums.

(2) Both rarefaction and Shannon-Wiener (*H'*) declined gradually from ~220 cm (~1.3 Ma). These decreasing patterns in community structure were generally the opposite of the increasing pattern in the abundance of benthic foraminifera across ~200 cm. Stilostomellidae and Pleurostomellidae decreased gradually after ~1.3 Ma and practically disappeared at ~0.7 Ma. These taxa became extinct during the Mid-Pleistocene Transition, whereas the earlier taxonomic loss of these taxa may explain the general decline in species diversity measures in core PC311. This timing roughly coincides with the enhanced zonal gradient of sea surface temperature between the eastern and western Equatorial Pacific Ocean.

(3) Stilostomellidae and Pleurostomellidae generally decreased upward with several fluctuations. In contrast, *Pseudoparrella obtusa*, a possible phytodetritus species, increased intermittently after ~1.3 Ma. In addition, the *Globocassidulina subglobosa–Globocassidulina ryukyuensis* plexus was abundant prior to ~1.5 Ma, whereas *Globocassidulina obtusa* became more common after ~1.4 Ma. The temporal decrease in Stilostomellidae and increase in *Astronion echolsi* may indicate the influence of the Upper Circumpolar Deep Water from the Southern Ocean-originated deep water on the shallower (lower bathyal) depth at our core site, rather than North Pacific Deep Water, across ~2 Ma. Thus, such a faunal transition can be explained by changes in global deep-water circulation and the enhanced east-west zonal gradient of sea surface temperature in the Equatorial Pacific Ocean.

Acknowledgements

We thank the shipboard crew of *R/V Onnuri* (Korean Institute of Ocean Science and Technology) for collecting a piston core PC311. We appreciate Akira Tsujimoto (Simane University) for his help taking SEM and light micrographs of planktonic foraminifera. We are indebted to Shungo Kawagata (Yokohama National University) for his suggestions regarding the taxonomy of benthic foraminifera. We also thank the associate editor (Kazuhiko Fujita) and reviewers (Bruce Hayward, Shun Chiyonobu and an anonymous reviewer) for their constructive comments to improve the manuscript. This work was supported by the Korea Institute of Ocean Science and Technology (KIOST) research program (PEA0182), Korea Institute of Marine Science & Technology (KIMST) funded by the Ministry of Oceans and Fisheries (RS-2023-00256330), and a part of the project titled 'Selection of prospective mining area for Co-rich ferromanganese crust in western Pacific seamounts: 3-D resource estimation and environmental impact evaluation', funded by the Ministry of Oceans and Fisheries (No. 20220509).

Supplementary materials

Supplementary figure 1. Temperature, salinity, and chlorophyll-a concentration in the surface water around our study area taken from Acker and Leptoukh (2007); Supplementary figure 2. Correlations of the dextral coiling ratios of Pulleniatina spp. between IODP Site U1486 (Pearson and Penny, 2021) and core PC311 (this study) with planktonic foraminiferal (PF) and calcareous nannofossil (CN) biohorizons. Error bars in the coiling plot represent 95% confidence interval; Supplementary figure 3. Stratigraphic variations of sea surface temperature and sea surface salinity at ODP Site 871 (Wang *et al.*, 2023); Supplemental document. Faunal References of planktonic foraminifera; Supplementary table 1. Occurrences of planktonic foraminifera in core 311; Supplementary table 2. Occurrences of calcareous nannofossils in core PC311; Supplementary table 3. Biohorizons of planktonic foraminifera and calcareous nannofossils in core PC311; Supplementary table 4. Occurrences of benthic foraminifera in core PC311™.

References

Altenbach, A. V., Pflaumann, U., Schiebel, R., Thies, A., Timm, S. and Trauth, M., 1999: Scaling percentages and distributional patterns of benthic Foraminifera with flux rates of organic carbon. *Journal of Foraminiferal Research*, vol. 29, p. 173–185.

Aubry, M.-P., 1984: *Handbook of Cenozoic Calcareous Nannoplankton*, 263 p. Micropaleontology Press, American Museum of Natural History, Washington DC.

Berggren, W. A., Hilgen, F. J., Langereis, C. G., Kent, D. V., Obradovich, J. D., Rafii, I. *et al.*, 1995a: Late Neogene chronology: new perspectives in high-resolution stratigraphy. *Geological Society of America Bulletin*, vol. 107, p. 1272–1287.

Berggren, W. A., Kent, D. V., Swisher, C. C. III and Aubry, M.-P., 1995b: A revised Cenozoic geochronology and chronostratigraphy. *In*, Berggren, W. A., Kent, D. V., Aubry, M.-P. and Hardenbol, J. *eds.*, *Geochronology, Time Scales and Global Stratigraphic Correlation*, p. 129–212. SEPM Special Publication, no. 54, SEPM, Claremore.

Burls, N. J., Fedorov, A. V., Sigman, D. M., Jaccard, S. L., Tiedemann, R. and Haug, G. H., 2017: Active Pacific meridional overturning circulation (PMOC) during the warm Pliocene. *Science Advances*, vol. 3, e1700156.

Buzas, M. A. and Gibson, T. G., 1969: Species diversity: benthonic foraminifera in western North Atlantic. *Science*, vol. 163, p. 72–75.

Eberwein, A. and Mackensen, A., 2006: Regional primary productivity differences off Morocco (NW-Africa) recorded by modern benthic foraminifera and their stable carbon isotopic composition. *Deep-Sea Research I*, vol. 53, p. 1379–1405.

Fedorov, A. V., Burls, N. J., Lawrence, K. T. and Peterson, L. C., 2015: Tightly linked zonal and meridional sea surface temperature gradients over the past five million years. *Nature Geoscience*, vol. 8, p. 975–980.

Feng, H., Tian, J., Lyle, M., Westerhold, T. and Wilkens, R., 2022: High resolution benthic foraminiferal $\delta^{18}O$ and $\delta^{13}C$ records at ODP site 807 over the past 5 Ma, Ontong Java Plateau: Evolution of North Pacific ventilation, Pliocene to Holocene. *Global and Planetary Change*, vol. 217, 103945.

Fillon, R. F., 1974: Late Cenozoic foraminiferal paleoecology of the Ross Sea, Antarctica. *Micropaleontology*, vol. 20, p. 129–151.

Gastaldello, M. E., Agnini, C., Westerhold, T., Drury, A. J. and Alegret, L., 2024: Unravelling changes in the productivity regime during the Late Miocene–Early Pliocene biogenic bloom: Insights from the western equatorial Pacific (IODP Site U1488). *Marine Micropaleontology*, vol. 191, 102395.

Gibbard, P. L. and Head, M. J., 2020: The Neogene Period. *In*, Gradstein, F. M., Ogg, J. G., Schmitz, M. D. and Ogg, G. M. *eds.*, *The Geologic Time Scale 2020*, vol. 2, p. 1217–1255. Elsevier, Amsterdam.

Gooday, A. J., 1994: The biology of deep-sea foraminifera: a review of some advances and their applications in paleoceanography. *Palaios*, vol. 9, p. 14–31.

Gooday, A. J., 2003: Benthic foraminifera (Protista) as tools in deep-water paleoceanography: a review of environmental influences on faunal characteristics. *Advances in Marine Biology*, vol. 46, p. 1–90.

Gooday, A. J., Nomaki, H. and Kitazato, H., 2008: Modern deep-sea benthic foraminifera: a brief review of their morphology-based biodiversity and trophic diversity. *In*, Austin, W. E. N. and James, R. H. *eds.*, *Biogeochemical Controls on Palaeoceanographic Environmental Proxies*, p. 97–119. Special Publication of Geological Society, vol. 303, Geological Society, London.

Hayward, B. W., Johnson, K., Sabaa, A. T., Kawagata, S. and Thomas, E., 2010: Cenozoic record of elongate, cylindrical, deep-sea benthic foraminifera in the North Atlantic and equatorial Pacific Oceans. *Marine Micropaleontology*, vol. 74, p. 75–95.

Hayward, B. W., Kawagata, S., Sabaa, A., Grenfell, H., van Kerkhoven, L., Johnson, K. *et al.*, 2012: The last global extinction (mid-Pleistocene) of deep-sea benthic foraminifera (Chrysalogoniidae, Ellipsoidinidae, Glandulonodosariidae, Plectofrondicularidae, Pleurostomellidae, Stilostomellidae), their late Cretaceous–Cenozoic history and taxonomy. *Cushman Foundation for Foraminiferal Research Special Publication*, vol. 43, p. 1–408.

Jones, R. W., 1994: *The Challenger Foraminifera*, 149 p. Oxford University Press, Oxford.

Jorissen, F. J., Fontanier, C. and Thomas, E., 2007: Paleoceanographical proxies based on deep-sea benthic foraminiferal assemblage characteristics. *In*, Hillaire-Marcel, C. and de Vernal, A. *eds.*, *Proxies in Late Cenozoic Paleoceanography*, p. 263–326. Elsevier, Amsterdam.

Kao, H.-Y. and Lagerloef, G. S. E., 2015: Salinity fronts in the tropical Pacific Ocean. *Journal of Geophysical Research: Oceans*, vol. 120, p. 1096–1106.

Kawagata, S., 1999: Late Quaternary bathyal benthic foraminifera from three Tasman Sea cores, southwest Pacific Ocean. *Science Reports of the Institute of Geoscience*, *University of Tsukuba*, *Section B*, *Geological Sciences*, vol. 20, p. 1–46.

Khim, B.-K., Kim, W., Hayashi, H., Kuwano, D., Routledge, C. M., Takata, H. *et al.*, 2005: Integrated chronostratigraphy of Magellan Seamount KC-7 in the western Pacific Ocean for Late Neogene paleoceanographic studies. *Newsletters on Stratigraphy*, vol. 58, p. 397–420.

Lam, A. R., Crundwell, M. P., Leckie, R. M., Albanese, J. and Uzel, J. P., 2022: Diachroneity rules the mid-latitudes: A test case using Late Neogene planktic foraminifera across the Western Pacific. *Geosciences*, vol. 12, 190.

Le Houedec, S., Meynadier, L. and Allègre, C. J., 2016: Seawater Nd isotope variation in the Western Pacific Ocean since 80 Ma (ODP 807, Ontong Java Plateau). *Marine Geology*, vol. 380, p. 138–147.

Li, Z. and Fedorov, A. F., 2022: Coupled dynamics of the North Equatorial Countercurrent and Intertropical Convergence Zone with relevance to the double-ITCZ problem. *Proceedings of the National Academy of Sciences*, vol. 119, e2120309119.

Loeblich, A. R. Jr. and Tappan, H., 1987: *Foraminiferal Genera and their Classification*, 970 p. Van Nostrand Reinhold, New York.

Lyle, M., Barron, J., Bralower, T. J., Huber, M., Lyle, A. O., Ravelo, A. C. *et al.*, 2008: Pacific Ocean and Cenozoic evolution of climate. *Review of Geophysics*, vol. 46, doi: 10.1029/2005RG000190.

Matsuoka, H. and Okada, H., 1989: Quantitative analysis of Quaternary nannoplankton in the subtropical Northwestern Pacific Ocean. *Marine Micropaleontology*, vol. 14, p. 97–118.

Miao, Q. and Thunnel, R. C., 1993: Recent deep-sea benthic foraminiferal distribution in the South China and Sulu Seas. *Marine Micropaleontology*, vol. 22, p. 1–32.

Motoi, T., Chan, W.-L., Minobe, S. and Sumata, H., 2005: North Pacific halocline and cold climate induced by Panamanian Gateway closure in a coupled ocean-atmosphere GCM. *Geophysical Research Letters*, vol. 32, doi: 10.1029/2005GL022844.

Nomura, R., 1983a: Cassodilinidae (Foraminiferida) from the Uppermost Cenozoic of Japan (Part 1). *Science Reports of Tohoku University*, *2nd Series (Geology)*, vol. 53, p. 1–101.

Nomura, R., 1983b: Cassodilinidae (Foraminiferida) from the Uppermost Cenozoic of Japan (Part 2). *Science Reports of Tohoku University*, *2nd Series (Geology)*, vol. 54, p. 1–93.

Nomura, R., 1995: Paleogene to Neogene deep-sea paleoceanography in the eastern Indian Ocean: benthic foraminifera from ODP Sites 747, 757 and 758. *Micropaleontology*, vol. 41, p. 251–290.

Nomura, R., 1999: Miocene Cassidulinid Foraminifera from Japan. *Paleontological Society of Japan*, *Special Papers*, no. 38, p. 1–69.

Okada, H. and Bukry, D., 1980: Supplementary modification and introduction of code numbers to the low-latitude coccolith biostratigraphic zonation. *Marine Micropaleontology*, vol. 5, p. 321–325.

Oksanen, J., Blanchet, G., Friendly, M., Kindt, R., Legendre, P., McGlinn, D. *et al.*, 2019: *Vegan: community ecology package. R package version* v. 2. 5-6 [online]. [Cited 1 September 2019]. Available from: http://cran.r-project.org/web/packages/vegan/index.html.

Pearson, P. N. and Penny, L., 2021: Coiling directions in the planktonic foraminifer *Pulleniatina*: A complex eco-evolutionary dynamic spanning millions of years. *PLoS ONE*, vol. 16, e0249113.

Perch-Nielsen, K., 1985: Cenozoic calcareous nannofossils. *In*, Bolli, H. M., Saunders, J. B. and Perch-Nielsen, K. *eds.*, *Plankton Stratigraphy*, p. 427–554. Cambridge University Press, Cambridge.

Pisias, N. G. and Moore, T. C. Jr., 1981: The evolution of the Pleistocene climate: a time series approach. *Earth and Planetary Science Letters*, vol. 52, p. 450–458.

Pujos, A., 1987: Late Eocene to Pleistocene medium-sized and small-sized "Reticulofenestrids". *In*, Stradner, H. and Perch-Nielsen, K. *eds.*, *International Nannoplankton Association, Vienna Meeting, 1985, Proceedings*, vol. 39, p. 239–277. Abhandlungen der Geologischen Bundesanstalt, Vienna.

R Development Core Team, 2020: *R: a language and environments for statistical computing* [online]. [Cited 22 June 2020]. Available from: http://www.R-project.org.

Raffi, I., Wade, B. S. and Pälike, H., 2020: The Neogene Period. *In*, Gradstein, F. M., Ogg, J. G., Schmitz, M. D. and Ogg, G. M. *eds.*, *The Geologic Time Scale 2020*, vol. 2, p. 1141–1215. Elsevier, Amsterdam.

Reid, J. L., 1965: Intermediate waters of the Pacific Ocean. *Johns Hopkins Oceanographic Studies*, no. 2, p. 1–85.

Reid, J. L., 1997: On the total geostrophic circulation of the Pacific Ocean: flow patterns, tracers, and transports. *Progress in Oceanography*, vol. 39, p. 263–352.

Saito, T., 1976: Geologic significance of coiling direction in the planktonic foraminifera *Pulleniatina*. *Geology*, vol. 4, p. 305–309.

Sato, T., Chiyonobu, S. and Hodell, D. A., 2009: Quaternary calcareous nannofossils datums and biochronology in the North Atlantic Ocean, IODP Site U1308. *In*, Channell, J. E. T., Kanamatsu, T., Sato, T., Stein, R., Alvarez Zarikian, C. A., Malone, M. J. *et al. eds.*, *Proceeding Integrate Ocean Drilling Program*, vols. 303 and 306, p. 1–9. Ocean Drilling Program, College Station.

Sato, T., Saito, T., Takahashi, H., Kameo, K., Sato, Y., Osato, C. *et al.*, 1998: Preliminary report on the geographical distribution of the cold water nannofossil *Coccolithus pelagicus* (Wallich) Schiller during The Pliocene to Pleistocene. *Journal of the Mining College*, *Akita University, Series A*, *Mining Geology*, vol. 8, p. 33–48.

Sato, T. and Takayama, T., 1992: A stratigraphically significant new species, *Reticulofenestra asanoi* (calcareous nannofossil). *In*, Ishizaki, K. and Saito, T. *eds.*, *Centenary of Japanese Micropaleontology*, p. 457–460. Terra Scientific Publishing Company, Tokyo.

Seo, I., Lee, Y. I., Kim, W., Yoo, C. M. and Hyeong, K., 2015: Movement of the Intertropical Convergence Zone during the mid-Pleistocene transition and the response of atmospheric and surface ocean circulations in the central equatorial Pacific. *Geochemistry*, *Geophysics*, *Geosystems*, vol. 16, p. 3973–3981.

Suhr, S. B. and Pond, D. W., 2006: Antarctic benthic foraminifera facilitate rapid cycling of phytoplankton-derived organic carbon. *Deep-Sea Research II*, vol. 53, p. 895–902.

Suhr, S. B., Pond, D. W., Gooday, A. J. and Smith, C. R., 2003: Selective feeding by foraminifera on phytodetritus on the western Antarctic Peninsula shelf: evidence from fatty acid biomarker analysis. *Marine Ecology Progress Series*, vol. 262, p. 153–162.

Takayama, T., 1978: III Calcareous nannoplankton. *In*, Takayanagi, Y. *ed.*, *Manual of Microfossil Studies*, p. 51–59. Asakura Books, Tokyo. (*in Japanese*)

Takayama, T. and Sato, T., 1987: Coccolith biostratigraphy of the North Atlantic Ocean, Deep Sea Drilling Project Leg 94. *Initial Reports. Deep Sea Drilling Project*, vol. 94, p. 651–702. U.S. Government Printing Office, Washington, DC.

Thomas, E., 2007: Cenozoic mass extinctions in the deep sea: what perturbs the largest habitat on Earth? *Geological Society of America, Special Paper*, vol. 424, p. 1–23.

Van Morkhoven, F. P. C. M., Berggren, W. A. and Edwards, A. S., 1986: Cenozoic cosmopolitan deep-water benthic foraminifera. *Bulletin Centres Recherches Exploration-Prodroduction Elf-Aquitaine Mémoire*, vol. 11, p. 1–421.

Wade, B. S., Pearson, P. N., Berggren, W. A. and Pälike, H., 2011: Review and revision of Cenozoic tropical planktonic foraminiferal biostratigraphy and calibration to the geomagnetic polarity and astronomical time scale. *Earth-Science Reviews*, vol. 104, p. 111–142.

Wang, X., Wang, Y., Dyez, K. A., Ravelo, A. C., Sun, C., Liu, F. *et al.*, 2023: Southward shift and intensification of the intertropical convergence zone in the North Pacific across the mid-Pleistocene transition. *Geophysical Research Letters*, vol. 50, e2023GL105983.

Wara, M. W., Ravelo, A. C. and Delaney, M. L., 2005: Conditions during the Pliocene warm period. *Science*, vol. 309, p. 758–761.

Wyrtki, K., 1974: Sea level and the seasonal fluctuations of the equatorial currents in the Western Pacific Ocean. *Journal of Physical Oceanography*, vol. 4, p. 91–103.

Young, J. R., 1998: Neogene. *In*, Bown P. R., *ed.*, *British Micropalaeontological Society Publications Series, Calcareous Nannofossil Biostratigraphy*, p. 225–282. Kluwer Academic Publisher, Cambridge.

Author contributions

HT was responsible for conducting the faunal analysis of benthic foraminifera of core PC311 and for writing the manuscript. HH and SH were also responsible for conducting the analyses of planktonic foraminifera and calcareous nannofossils, respectively, and for biostratigraphic age inferences. RN assisted HT with the faunal analysis of benthic foraminifera. CMY was in charge of taking sediment core PC311 during the expedition. BKK designed the research, contributed to writing the manuscript, and managed the discussion for consensus. All authors approved the submission of the manuscript.